HHS Public Access

Author manuscript

J Cogn Neurosci. Author manuscript; available in PMC 2021 May 05.

Published in final edited form as:

J Cogn Neurosci. 2020 August ; 32(8): 1536–1549. doi:10.1162/jocn_a_01562.

White Matter Microstructure Predicts Focal and Broad Functional Brain Dedifferentiation in Normal Aging

Jenny R. Rieck[1], **Karen M. Rodrigue**[2], **Denise C. Park**[2], **Kristen M. Kennedy**[2]

[1]Rotman Research Institute, Toronto, ON, Canada

[2]The University of Texas at Dallas

Abstract

Ventral visual cortex exhibits highly organized and selective patterns of functional activity associated with visual processing. However, this specialization decreases in normal aging, with functional responses to different visual stimuli becoming more similar with age, a phenomenon termed “dedifferentiation.” The current study tested the hypothesis that age-related degradation of the inferior longitudinal fasciculus (ILF), a white matter pathway involved in visual perception, could account for dedifferentiation of both localized and distributed brain activity in ventral visual cortex. Participants included 281 adults, ages 20–89 years, from the Dallas Lifespan Brain Study who underwent diffusion-weighted imaging to measure white matter diffusivity, as well as fMRI to measure functional selectivity to viewing photographs from different categories (e.g., faces, houses). In general, decreased ILF anisotropy significantly predicted both focal and broad functional dedifferentiation. Specifically, there was a localized effect of structure on function, such that decreased anisotropy in a smaller mid-fusiform region of ILF predicted less selective (i.e., more dedifferentiated) response to viewing faces in a proximal face-responsive region of fusiform. On the other hand, the whole ILF predicted less selective response across broader ventral visual cortex for viewing animate (e.g., human faces, animals) versus inanimate (e.g., houses, chairs) images. This structure–function relationship became weaker with age and was no longer significant after the age of 70 years. These findings indicate that decreased white matter anisotropy is associated with maladaptive differences in proximal brain function and is an important variable to consider when interpreting age differences in functional selectivity.

INTRODUCTION

Ventral visual cortex encompasses regions of occipito-temporal cortex that are uniquely specialized for the identification and recognition of visual stimuli (Grill-Spector & Malach, 2004). Abundant early neuroimaging work has demonstrated selective and localized brain response when viewing certain categories of images (e.g., face-selective regions of fusiform gyrus; Epstein, Harris, Stanley, & Kanwisher, 1999; Kanwisher, McDermott, & Chun, 1997; Haxby et al., 1994), with further evidence for category-specific patterns of activity distributed broadly across ventral visual cortex (O’Toole, Jiang, Abdi, & Haxby, 2005;

Reprint requests should be sent to Kristen M. Kennedy, Center for Vital Longevity, School of Behavioral and Brain Sciences, The University of Texas at Dallas, 1600 Viceroy Dr., Dallas, TX 75235, or via kristen.kennedy1@utdallas.edu.

Haxby et al., 2001). Moreover, one of the largest distinctions in ventral visual cortex is characterized by activity in lateral and superior regions when viewing animate images (e.g., faces, animals, bodies) versus medial and inferior regions when viewing inanimate images (e.g., tools, houses; Proklova, Kaiser, & Peelen, 2016; Grill-Spector & Weiner, 2014; Sha et al., 2014; Haxby et al., 2011). Researchers have proposed that categorical representations in ventral visual cortex are multifaceted and exist at both a focal and broad level with smaller specialized regions, like face-selective fusiform, associated with narrow category distinctions (i.e., “face” vs. “house”) that are nested within larger functional regions involved in superordinate distinctions (i.e., “animate” vs. “inanimate”; Grill-Spector & Weiner, 2014).

With advanced age, these highly specialized and unique representations associated with processing different visual stimuli become less distinct or “dedifferentiated” (Park et al., 2004; Grady et al., 1994; see Koen & Rugg, 2019, for a review). Specifically, with increasing age, localized regions of fusiform specialized for face processing show a broadened response by activating to nonface stimuli (Park et al., 2004, 2012). Furthermore, the distributed patterns of brain activity when viewing faces versus other inanimate stimulus categories (e.g., houses or chairs) become more similar in older age (Burianová, Lee, Grady, & Moscovitch, 2013; Carp, Park, Polk, & Park, 2011). Importantly, this neural dedifferentiation has been associated with poorer performance on measures of fluid processing (Rieck, Rodrigue, Kennedy, Devous, & Park, 2015; Park, Carp, Hebrank, Park, & Polk, 2010) and face matching (Burianová et al., 2013), suggesting that individual differences in brain activity underlying visual perception may account for cognitive aging processes (Park & Reuter-Lorenz, 2009).

One possible explanation for dedifferentiation of functional activity in aging is degradation of the underlying white matter structure. Aging is characterized by dysmyelination and alteration of white matter fiber organization, which, in turn, likely interferes with the transfer and function of neural signals in gray matter (Daselaar et al., 2015; Barnes & McNaughton, 1980). Prior work has examined how measures of white matter microstructure explain age differences in: task-evoked functional response (Hakun, Zhu, Brown, Johnson, & Gold, 2015; Zhu, Johnson, Kim, & Gold, 2015; Burzynska et al., 2013; de Chastelaine, Wang, Minton, Muftuler, & Rugg, 2011; Madden et al., 2007; Persson et al., 2006; see Warbrick, Rosenberg, & Shah, 2017; Bennett & Rypma, 2013, for reviews), modulation of functional response amplitude (Webb, Hoagey, Foster, Rodrigue, & Kennedy, 2020; Brown, Hakun, Zhu, Johnson, & Gold, 2015), and functional connectivity between cortical regions (Davis, Kragel, Madden, & Cabeza, 2012; Chen, Chou, Song, & Madden, 2009). However, the impact of age-related white matter degradation on highly specialized functional activity (as found in the ventral visual cortex) is unclear.

Here, we examine the impact of aging on the relationship between category-selective activations in ventral visual cortex and underlying microstructure of the inferior longitudinal fasciculus (ILF), the principal white matter pathway that connects occipital cortex to inferior and medial-temporal brain regions (Catani, Jones, Donato, & Ffytche, 2003). Behavioral studies find that ventral–temporal white matter (including the ILF) is important for a variety of different visually related cognitive processes, including reading ability (Yeatman,

Dougherty, Myall, Wandell, & Feldman, 2012; Ellmore et al., 2010), recognition of visual stimuli (Tavor et al., 2014; Sasson, Doniger, Pasternak, & Assaf, 2010; Davis et al., 2009), and face discrimination (Thomas et al., 2008). Furthermore, previous work has identified ILF fibers that serve as direct connections between face-selective functional regions of ventral visual cortex (Liu, Hildebrandt, Meyer, Sommer, & Zhou, 2020; Weiner et al., 2016; Pyles, Verstynen, Schneider, & Tarr, 2013; Gschwind, Pourtois, Schwartz, Van De Ville, & Vuilleumier, 2012; Saygin et al., 2012), suggesting that this white matter structure supports the specialized functional activity in ventral visual cortex.

We hypothesized that age-related degradation of ILF would account for functional dedifferentiation during visual processing at both the focal and distributed level. To test this hypothesis, we utilized two brain activation measures of dedifferentiation, also referred to as "selectivity": (1) selectivity for faces in localized face-selective regions of fusiform gyrus (i.e., fusiform face area [FFA]) and (2) broad selectivity for animacy across the entire ventral visual cortex. In general, functional selectivity describes the degree to which a specific region of cortex shows increased and selective response during one experimental condition (i.e., viewing faces) but not another (i.e., viewing houses). This hypothesis was tested in the Dallas Lifespan Brain Study, with adults ranging in age from 20 to 89 years, allowing the exploration of the relationship between white matter and neural dedifferentiation across the adult lifespan, including often excluded groups of middle-aged adults and very old aged adults (i.e., > 80 years). We also considered that younger adults would vary in ILF integrity and that an effect of decreased anisotropy in ILF would be maintained, even after age was controlled.

METHODS

Participants

Participants consisted of a subsample from the Dallas Lifespan Brain Study who underwent passive viewing of categories of photographs during fMRI and also had diffusion tensor imaging (DTI) data collected (n = 299). Participants' informed consent was obtained in accordance with protocol approved by The University of Texas at Dallas and the University of Texas Southwestern Medical Center. Participants were screened to be right-handed and fluent English speakers with normal or corrected-to-normal vision (at least 20/30), and if necessary, vision was corrected using MRI-compatible corrective lenses during the fMRI session. Participants were additionally screened to be cognitively intact (Mini-Mental Status Exam ≥ 26; Folstein, Folstein, & McHugh, 1975), with no history of neurological or psychiatric conditions, head trauma, drug or alcohol problems, or significant cardiovascular disease. Participants with outlier data points (detailed in Statistical Analysis section; n = 18) for each neural measure were identified and excluded from analyses, resulting in a final sample size of 281 (see Table 1 for sample demographics).

MRI Acquisition

Participants were scanned on a single Philips Achieva 3T whole-body scanner equipped with an eight-channel head coil. DTI volumes were acquired with the following parameters: repetition time (TR) = 4410 msec, echo time (TE) = 51 msec, flip angle = 90°, field of view

(FOV) = 224 × 149 × 224, *XY* matrix = 112 × 110, 50 slices per volume, 30 directions were acquired at $b = 1000$ sec/mm^2, plus a b0 non-diffusion-weighted image. BOLD fMRI data were acquired using a T2*-weighted EPI sequence with 43 interleaved axial slices (in a 64 × 64 matrix) acquired parallel to the AC–PC line with the following parameters: 3.4 × 3.4 × 3.5 mm^3 voxels, FOV = 220 mm, TE = 25 msec, TR = 2 sec, flip angle = 80°. High-resolution anatomical images (used to coregister anatomical masks to native diffusion and functional space) were collected with a T1-weighted MP-RAGE sequence with the following parameters: 160 sagittal slices, 1 × 1 × 1mm^3 voxels;256×256×160matrix,FOV=220mm,TE=3.76 msec, TR = 8.19 msec, flip angle = 12°.

Diffusion Tensor Imaging

DTI Processing—Diffusion volumes were processed using the FMRIB's Diffusion Toolbox (FDT) in FSL (Behrens, Berg, Jbabdi, Rushworth, & Woolrich, 2007; Behrens et al., 2003). First, volumes underwent eddy current correction to correct for distortions caused by eddy currents in the gradient coils, as well as simple head motion during image acquisition by using an affine registration to a reference volume (using FLIRT). Second, the images were skull stripped using Brain Extraction Tool. Next, diffusion tensors were fit on corrected data using *dtifit* to create a voxel-wise map of the three primary diffusion directions (i.e., λ_1, λ_2, and λ_3) for each participant.

The three diffusion directions were used to compute our primary measure of white matter microstructure: fractional anisotropy (FA), which describes the ratio of diffusion in the primary direction ($\lambda 1$ or axial diffusivity [AD]) relative to perpendicular directions (λ_2 and λ_3 or radial diffusivity [RD]). Because FA is a composite index of diffusivity in all directions, it is important to consider AD and RD when interpreting differences in white matter microstructure (e.g., decreased AD coupled with increased RD could result in decreased FA). Therefore, in the current study, significant effects of FA were further explored by also examining the contribution of AD and RD to the statistical models.

Isolating White Matter Structures—The primary white matter pathway of interest was the ILF, and we also isolated a smaller mid-fusiform portion of ILF for follow-up analyses. Four additional white matter structures were identified to serve as control white matter regions: the superior longitudinal fasciculus (SLF), the uncinate fasciculus (UF), and the genu and splenium of the corpus callosum.

Probabilistic tractography was conducted to isolate the three bilateral association white matter pathways (ILF, SLF, and UF), separately in each participant's native space using FDT in FSL (Behrens et al., 2007). First, diffusion parameters were estimated at each voxel using *bedpostX*, which generates a probability distribution function of the primary diffusion directions. Then, to determine connectivity between voxels, *probtrackX* was used to estimate the distribution of connections between the seed regions (i.e., origin) and waypoint (i.e., inclusion) regions (described below). The output from this step was a connectivity value for each voxel that represents the number of fibers that passed through that voxel.

All masks were constructed in standard Montreal Neurological Institute (MNI) space and then backwarped to each participant's native diffusion space, and all seed and waypoint

regions were rectangular masks—6 mm deep (anterior–posterior/coronal), 18 mm wide (left–right/sagittal), and 28 mm high (dorsal–ventral/axial)—constructed separately for the left and right hemispheres. A midline exclusion mask was also included to eliminate fibers that crossed hemisphere.

ILF seed masks (i.e., tract origins) were created in occipital white matter, 24 mm anterior to the most posterior slice of the brain, and a single waypoint mask was created in temporal white matter, 50 mm anterior to the seed mask. Seed and waypoint masks were positioned such that they were centered around anterior–posterior oriented white matter as evident on the MNI template (see Figure 1A for an illustration of ILF masks and the resulting pathway for a representative participant in cyan). For the SLF, seed masks were constructed in superior white matter on the most posterior coronal slices in which the splenium of the corpus callosum was visible on the MNI template. Two SLF waypoint masks were constructed 22 and 44 mm anterior to the seed mask. For the UF, seed masks were positioned in anterior temporal white matter, 30 mm posterior to the tip of the temporal pole. One waypoint mask was placed in the white matter of the anterior floor of the external capsule.

The resulting white matter tracts were thresholded at 15% of the maximum connectivity value, which ensured that tracts only included those voxels with a high likelihood of being connected to the seed and waypoint regions (following Bennett, Motes, Rao, & Rypma, 2012). All tracts were then visually inspected to verify that the backwarping of the seed and waypoint regions to native diffusion space resulted in proper tracking. Thresholded tracts were binarized, and mean FA, AD, and RD were extracted and averaged across hemispheres.

To localize fibers within the genu (anterior portion) and splenium (posterior portion) of the corpus callosum, rather than including pericallosal fibers, ROIs were hand-traced on the T2-weighted (b0) baseline image for each participant in their native diffusion space with high reliability (intraclass correlation coefficient > .95). Each region was traced with a stylus on an LCD digitizing tablet using Analyze v12.0 software (Mayo Clinic). The genu and splenium were both traced on the slices in which they were optimally visible, for each participant with at least three slices included per structure. For each participant, diffusivity measure (e.g., FA, AD, RD) were extracted from the hand-traced genu and splenium and averaged across slices for each structure.

Finally, a smaller portion of ILF in mid-fusiform (proximal to the functional FFA) was identified to test regional specificity of structure–function relationships. Because the decision to examine mid-fusiform ILF was post hoc, the region was identified in an unbiased manner via a group-level analysis of the fMRI data. Specifically, rectangular masks were created in MNI space (28 mm ×12 mm × 18 mm, similar to the ILF tractography seed and waypoint masks) that were centered around the left ($Y = -43$) and right ($Y = -48$) Y values for the peak clusters from a group-level analysis of functional activity for faces > houses (illustrated in Figure 2C). These MNI masks were then backwarped to each participant's native diffusion space and overlaid with their ILF pathway generated from tractography. Mean FA was extracted from the conjunction of the backwarped mask and the ILF pathway to create a measure of mid-fusiform ILF microstructure in roughly equivalent anatomical

regions for each participant (confirmed via visual inspection) that was proximal to functional activity in FFA. A visualization of this mid-fusiform segment for one participant can be found in Figure 1A (yellow portion of ILF).

Functional Magnetic Resonance Imaging

Visual Stimuli and Task Design—While in-scanner, participants were instructed to view images from six categories: human faces, primates, cats, houses, chairs, and phase-scrambled control stimuli. Each category was composed of 64 grayscale photographs (400 pixels wide × 300 pixels tall), and cat stimuli were made up of 32 domestic cat and 32 wild cat photographs. The images of human faces were taken from our published face library (Kennedy, Hope, & Raz, 2009; Minear & Park, 2004). Animal photographs (primates, domestic cats, and wild cats) were taken from the Internet and cropped so that the animal's face was clearly visible. Like the human faces, only animal images with front-facing and neutral expressions were chosen. Houses were photographed from various locations across the United States. The photographs of chairs were taken from furniture websites. Control images were created by scrambling the phase information in all the experimental stimuli so that the spatial frequency information was preserved, but the visual information was meaningless.

Visual stimuli were presented in a block design across two 7-min runs. There was a 10-sec fixation screen at the beginning and end of each run to allow brain tissue magnetization to reach a steady state and to allow for participants to become acclimated to the noise of the scanner. Within each run, 24 blocks (four blocks from the six categories) were presented in pseudorandom order. Within each block, there were eight images randomly selected from the same category so that each image was only presented one time. Individual images were presented for 2 sec each with no interstimulus interval. Participants were not required to make any response during the scan but were instructed to pay attention to each image. A subset of data from this task (i.e., the human and house viewing conditions) have been discussed in previous work (Park et al., 2012).

fMRI Processing—Individual participant's time series data were preprocessed with Statistical Parametric Mapping 8 (SPM8; Wellcome Department of Cognitive Neurology). First, images were corrected for differences in slice time acquisition. Next, individual volumes were corrected for within-run participant movement. Finally, images were smoothed with an isotropic 8-mm^3 FWHM Gaussian kernel. For the current study, the primary analysis of the fMRI data was conducted in participant native space to ensure the least amount of processing before analysis. However, an additional pipeline was run, which included a spatial normalization to a standardized MNI template before the smoothing step to ensure that warping the data to a standard space did not differ from the analysis conducted in native space.

First-level statistics were conducted using the general linear model in SPM8 to model BOLD response to each of the six image categories viewed in scanner: human faces, primates, cats, houses, chairs, and scrambled. For the current study, additional first-level models were conducted to estimate neural response to animate (human, primate, and cat)

and inanimate (house and chair) categories. In all models, motion parameters for each individual were also included as nuisance regressors to control for individual differences in movement across the scanning session. The resulting parameter estimates (β-weights) from the first-level models quantified how well functional activity in each voxel corresponded to a predicted neural response for that condition, thereby providing an estimate of BOLD response to each experimental condition.

Quantifying Functional Measures of Dedifferentiation—For the current study, two indices of functional dedifferentiation, also referred to as "selectivity," were examined: (1) functional selectivity for faces in face-selective regions of fusiform gyrus (e.g., FFA) and (2) broad functional selectivity for animacy across the entire ventral visual cortex.

To quantify face selectivity, we focused on activation patterns in the FFA, as this is the region of the core face network that shows the strongest age-related dedifferentiation compared with other regions of the face network (e.g., occipital face area, STS; Park et al., 2012). Following Park et al. (2012), for each participant, left and right FFA were identified within participant native space by isolating a ~200 mm^2 contiguous region around the peak voxel in fusiform gyrus that evoked significant response to viewing human faces versus scrambled images (FFA voxels that have been mapped to a common space are illustrated in Figure 2C). Within the functionally defined FFA, neural selectivity was quantified as the average difference in neural response to human faces compared with houses (more details can be found in Park et al., 2012). For the current study, FFA selectivity measurements were averaged for left and right hemispheres.

A second index of selectivity was also computed based on prior work demonstrating widespread differences in functional representations associated with animacy (Proklova et al., 2016; Grill-Spector & Weiner, 2014; Sha et al., 2014; Haxby et al., 2011). For the current study, selectivity for animacy was quantified by calculating the similarity between neural response to animate images (human, primate, and cat) and inanimate images (houses and chairs) using Euclidian distance, which is a measure of the magnitude of difference in neural response to different conditions across many voxels (Kriegeskorte, Mur, & Bandettini, 2008); a group-level contrast of animacy mapped to a common space is illustrated in Figure 2D).

Ventral visual cortex was identified for each participant using a participant-specific anatomical mask in conjunction with a functionally derived mask that isolated voxels in the ventral visual mask that showed significant response to any of the visual stimuli. Specifically, an anatomical mask of the ventral visual pathway was backwarped to participant native space using bilateral regions derived from the Automated Anatomical Labeling template (Tzourio-Mazoyer et al., 2002), specifically, calcarine sulcus, cuneus, lingual gyrus, inferior occipital gyrus, fusiform gyrus, parahippocampal gyrus, inferior and middle temporal gyrus, and temporal. Although not all of these regions are necessarily part of the "ventral visual pathway," they were selected to encompass the large swathe of cortical regions to which ILF projects in addition to functional regions involved in visual processing. Second, a functional mask was generated for each individual to isolate voxels within the ventral visual pathway that were responsive to visual input. Following O'Toole et al. (2014),

the functional mask was defined as those voxels within the ventral visual cortex that varied significantly across the six stimulus conditions as determined by an ANOVA F test. For the current study, the significance threshold was set to $p < .00001$ (O'Toole et al., 2014). Relaxing or increasing the significance threshold for the functional masks did not alter the results reported here.

Statistical Analysis

Outliers were removed from the sample by identifying those participants who evidenced outlier data points for any of the three primary brain variables of interest: ILF FA, FFA face selectivity, and ventral visual animacy selectivity. To ensure outlier removal was not influenced by normal aging effects, first age was regressed out of each brain variable of interest. Outliers were identified as those data points outside 1.5 times the interquartile range for the standardized residuals (after accounting for age). Eighteen total outliers were identified (ILF FA, $n = 5$; face selectivity, $n = 7$; animacy selectivity outliers, $n = 5$; both face and animacy selectivity, $n = 1$), for a final sample of $n = 281$.

Using R (R Core Team), several hierarchical regression models were conducted to examine the predictive effect of white matter microstructure on the different functional measures of selectivity. For each hierarchical regression, age was entered first, followed by FA for the control white matter regions (i.e., SLF, UF, genu, and splenium), and finally, ILF FA (the white matter pathway of interest). This analysis allowed us to determine if ILF microstructure predicted differences in functional selectivity beyond the effect of aging and controlling for white matter FA in other brain regions. Because the animacy measure was derived across a large region of ventral visual cortex in each individual's native space, the size of each individual's ventral visual area (as computed through their anatomically derived mask; range = 4769–7744 voxels in size, mean number of voxels = 5893) was also included as a nuisance covariate in each model to ensure that results were not influenced by individual differences in ventral visual size.

The regression models also allowed us to examine the shared (i.e., R^2) and unique (i.e., η^2) variance for each of the predictors to understand the age and ILF microstructure contributions to the overall model. For the highest level regression model, we also included Age × ILF microstructure interactions to examine how age might be modulating the relationship between white matter microstructure and functional selectivity. For models in which mean FA in ILF was found as a significant predictor, additional regressions were conducted (with predictors from the highest level significant hierarchical regression model) using other indicators of white matter diffusivity (i.e., AD and RD) to determine which diffusion metrics accounted for the effect of FA.

RESULTS

Age Effects on Structural and Functional Measures

The association of each structural and functional measure to age was individually assessed to establish that the usual sensitivity to aging was observed for each marker. As expected, with increasing age, diffusion in ILF was more isotropic as evident by the decrease in FA

values ($r = -.57$, $p < .001$), suggesting that integrity in ILF degrades with increasing age (Figure 1B). Age-related decreases in FA were characterized by a quadratic effect of age on AD ($r^2 = .10$, $p < .001$; Figure 1C) and linear effect of age on RD ($r = -.61$, $p < .001$; Figure 1D). Specifically, participants of ages 20–51 years show age-related increases in RD ($r = .31$, $p < .001$) and slight decreases in AD ($r = -.32$, $p < .001$). On the other hand, participants of ages 52–89 years showed age-related increases in both RD ($r = .42$, $p < .001$) and AD ($r = .30$, $p < .001$), which might be suggestive of a more severe pattern of degradation in adults over the age of 52 (Bennett, Madden, Vaidya, Howard, & Howard, 2010; Burzynska et al., 2010).

Both functional measures of selectivity showed decreases with increasing age (Figure 2). Specifically, in face-selective regions of fusiform gyrus (i.e., FFA), the difference in neural response to faces compared with houses was decreased in older age ($r = -.25$, $p < .001$; Figure 2A). Likewise, across the ventral visual cortex, the similarity of response between animate and inanimate images was decreased in older age ($r = -.27$, $p < .001$; Figure 2B).

Structure–Function Associations

Hierarchical regression models were conducted in which age and white matter metrics and nuisance covariates were entered to predict the two different measures of functional selectivity (i.e., face selectivity or animacy).

Face Selectivity—The first set of models predicted selectivity for faces versus houses in FFA and found that older age predicted decreased face selectivity ($\Delta R^2 = .062$, $p < .001$). However, adding mean FA of the ILF to the model (after controlling for age and FA in nonpreferred white matter pathways) did not significantly increase the amount of variance explained by the model ($\Delta R^2 = .002$, $p = .42$; Table 2A).

Given that the ILF is a fairly long fiber pathway, (i.e., up to 10 cm in length; Catani et al., 2003) and the FFA regions identified in the current study were roughly 8-mm spheres, it is possible that the size scale difference between the two measures accounted for the lack of the relationship between FA and face selectivity in FFA. Therefore, an additional regression model was conducted to determine if FA in a more local (i.e., mid-fusiform) portion of ILF was a better predictor of selectivity than FA averaged across the whole ILF pathway (see Methods for details on how this region was delineated). Specifically, left and right mid-fusiform FA was averaged and entered in a hierarchical regression model (after age, control regions FA, and whole ILF FA) to predict selectivity for faces within FFA.

This analysis revealed that decreased FA within the mid-fusiform region of ILF predicted decreased face selectivity within FFA ($\beta = 3.33$, $F(1, 273) = 6.43$, $p = .012$, $\eta^2 = .023$), even when accounting for age, other white matter regions, and whole ILF FA ($\Delta R^2 = .022$, $p = .012$; see Figure 3 for an illustration of this association).[1] Examining the unique variance (i.e., η^2) explained by each predictor in this model revealed that age accounted for 3.8% and

[1]To note, mid-fusiform FA remained predictive of FFA selectivity after also accounting for FA in two other segments of ILF more distal from FFA (one approximately 15 mm posterior and one approximately 15 mm anterior), $F(1,272) = 4.67$, $p = .032$, suggesting that these effects are specific to mid-fusiform ILF due to its proximity to the functional ROI, rather than due to inherent regional differences in FA values along the ILF.

mid-fusiform FA accounted for 2.3% of the total model variance (9.2%). These findings indicate that, even though both age and white matter have unique contributions to individual differences in FA selectivity, together these variables explain more variance than alone (Table 2A). Including an interaction term between age and mid-fusiform FA for this final model did not result in a significant interaction, $F(1, 272) = 0.266$, $p = .606$, nor did it explain more variance than the previous model ($\Delta R^2 = .001$, $p = .606$).

Two additional regression models were conducted using AD and RD, respectively, for each white matter region. These models demonstrated that the association between decreased white matter microstructure in mid-fusiform and decreased face selectivity in FFA was characterized by increased RD ($R^2 = .095$, $F(1, 273) = 3.97$, $p = .047$, $\eta^2 = .015$; Table 2B) and decreased AD ($R^2 = .099$, $F(1, 273) = 15.24$, $p < .001$, $\eta^2 = .053$; Table 2C) when accounting for age and control region diffusivity measures.

Animacy—The second set of hierarchical regression models predicted selectivity for animacy across ventral visual cortex. As expected, age was a significant predictor of selectivity for animacy ($\Delta R^2 = .071$, $p < .001$). Adding FA in control white matter regions ($\Delta R^2 = .006$, $p = .788$) and ventral visual volume size ($\Delta R^2 = .001$, $p < .583$) did not explain significantly more variance in neural selectivity. When accounting for all of these variables, whole ILF FA remained a significant predictor of neural selectivity for animacy ($\beta = 10.70$, $\Delta R^2 = .037$, $p < .001$; Table 3A); specifically, decreased white matter FA in ILF predicted decreased selectivity across ventral visual cortex.

Adding an Age × ILF FA term to this model again explained more variance than the previous step ($\Delta R^2 = .015$, $p = .031$) and also resulted in a significant interaction, $F(1, 272) = 4.66$, $p = .032$ (Table 3A), indicating that the association between ILF white matter and broad functional selectivity to animacy was age-dependent. Because both age and ILF FA were continuous variables, we used a simple slopes analysis (Preacher, Curran, & Bauer, 2006; Johnson & Fay, 1950) to examine how age modulated the relationship between structure and function. Specifically, we computed the slope of the relationship between ILF FA and ventral visual selectivity for the mean age in our sample (54 years), as well as 1 standard deviation above (74 years) and below (34 years). The simple slopes analysis revealed that strength of the relationship between whole ILF FA and broad functional selectivity became weaker with increasing age (β_{Age} 34 = 15.33, β_{Age} 54 = 10.77, β_{Age} 74 = 6.21; Figure 4A). Furthermore, using the Johnson–Neyman approach to examine the structure–function slopes across the entire lifespan confirmed that the relationship between ILF FA and functional selectivity was no longer significant after about the age of 70 years (Figure 4B, dotted vertical line).

Two additional regression models were conducted using AD and RD for each white matter region. These models indicated that decreased selectivity for animacy was predicted by increased RD ($R^2 = .137$, $F(1, 272) = 10.52$, $p = .001$, $\eta^2 = .037$; Table 3B), with no relationship found for AD ($R^2 = .118$, $F(1, 272) < 1$, $p = .527$, $\eta^2 = .002$; Table 3C). As with FA, the Age × ILF RD interaction was significant, $F(1, 272) = 4.51$, $p = .035$, $\eta^2 = .016$. A simple slopes analysis of the Age × RD interaction found that the relationship between white matter microstructure and ventral visual selectivity weakened with age (β_{Age} 34 = −13772,

β_{Age} 54 = −9750; age 74, β_{Age} 74 = −5727) and became nonsignificant after the age of 72 years.

DISCUSSION

This work provides new evidence of a direct relationship between ILF microstructure properties and functional selectivity in ventral visual cortex during visual perception. Specifically, decreased white matter anisotropy in ILF corresponded to less selective activation for animacy across the ventral visual cortex, independent of the effect of age. This effect was not found when trying to predict neural selectivity for faces within a specialized region of the face processing network. However, white matter anisotropy within a smaller and more localized portion of the ILF did predict functional selectivity in FFA. These results suggest that whole ILF white matter may be a stronger predictor of broad differences in selectivity across the entire ventral visual cortex, whereas more focal regions of ILF may be a stronger predictor of dedifferentiation of specialized face processing.

Whole ILF Microstructure Predicts Broad but Not Focal Measures of Neural Selectivity

The ILF is a fairly long fiber pathway that interconnects many areas of cortex between the occipital and temporal poles (Catani et al., 2003)—essentially along what is considered the ventral visual stream—and it is clear from behavioral studies that the ILF is involved in a variety of visually dependent cognitive processes, including reading ability (Yeatman et al., 2012; Ellmore et al., 2010), recognition of visual stimuli (Tavor et al., 2014; Sasson et al., 2010; Davis et al., 2009), and speed of processing (Bennett et al., 2012; Turken et al., 2008). Yet, it is only more recently that researchers have examined how white matter integrity in ILF relates to functional activity during visual processing. Both Gschwind et al. (2012) and Pyles et al. (2013) report that white matter fibers connecting specialized regions of the face processing network overlap with a portion of the ILF, suggesting that some fibers within ILF are important for transmitting neural activity related to face perception.

However, in the current study, no relationship was found between face selectivity in FFA and average FA of the entire ILF pathway, suggesting simply averaging the values for the entire tract—a common practice in DTI work (Bennett et al., 2012; Burzynska et al., 2010)—may not be the most sensitive predictor of brain activity within a small and localized region of the ventral visual pathway. Rather, FA within a more proximal region of ILF (mid-fusiform gyrus) was found to be the best predictor of face selectivity within FFA, suggesting that fibers within middle fusiform portions of the ILF may subserve specialized neural activity in face-selective regions of cortex. Earlier behavioral work reports a selective association between inferior fronto-occipital fasciculus (IFOF; a fiber pathway passing through fusiform to frontal regions of the extended face-network) and better face discrimination, particularly for more difficult judgments, whereas ILF showed no such relationship (Thomas et al., 2008). Given that IFOF and ILF show substantial spatial overlap in fusiform regions (Liu et al., 2020; Pyles et al., 2013), it is possible that our mid-fusiform subsection contains fibers from both pathways, which might explain the specific relationship we find between mid-fusiform FA and FFA face selectivity. Future work is needed to examine a dissociation of

mid-fusiform ILF and IFOF in predicting face selectivity in both core and extended regions of the face network.

On the other hand, whole ILF FA was found to be a significant predictor of selectivity for animacy across a large area of ventral visual cortex. Therefore, as a whole, white matter fibers of the ILF may subserve basic visual processing involved in superordinate category distinction within ventral visual pathway. Together, these results suggest that white matter exerts a local effect on neural activity, such that higher anisotropy in a small portion of ILF better predicts functional activity in proximal regions of cortex, whereas the entire ILF predicts broad differences in activity across ventral visual cortex. Although it is important to note that no standard exists for testing different gradients along white matter pathways using probabilistic tractography (see Yeh, Badre, & Verstynen, 2016), the current findings illustrate the utility in segmenting major white matter structures when corresponding functional regions are small and localized.

Different Properties of White Matter Microstructure Predict Functional Selectivity

The current study used mean tract FA as the primary index of white matter microstructure to predict functional selectivity. FA is a scalar measure that describes the relationship between the rates of water diffusion parallel to the primary direction of diffusion (AD) relative to diffusion in perpendicular directions (RD). Therefore, although FA is a useful measure for describing overall shape and orientation of diffusion, it is also interesting to consider how changes in both primary (AD) and perpendicular (RD) diffusivity may be accounting for differences in FA. In general, studies examining effects of age on white matter find that age-related decreases in FA can be due to relative changes in both axial and radial diffusion. Specifically, decreased FA has been accounted for by three different patterns: (1) increased RD only, which may indicate dysmyelination of the axonal sheath; (2) increased RD and AD, which may indicate a more severe dysmyelination; and (3) increased radial and substantial decreases in AD, which may indicate damage to the white matter axons (Bennett et al., 2010), although it is important to keep in mind that these are proxy metrics.

In the current study, decreased FA in middle fusiform ILF predicted decreased selectivity for faces in FFA, and additional analyses found that decreased selectivity was also predicted by increased RD and decreased AD (Pattern 3), independent of the effect of age. This pattern of increased RD and decreased AD may indicate that face selectivity in fusiform is sensitive to the pattern of diffusivity in nearby white matter, which may be characterized by slight alterations to axonal cellular boundaries. These results suggest that white matter in middle fusiform ILF may be more susceptible to more severe forms of degradation, and this in turn may impede functional response in nearby cortex. To note, the associations between white matter metrics and neural selectivity persisted beyond the effect of age; therefore, differences in diffusivity likely represent subtle individual differences, rather than age-pecific or age-dependent white matter degradation.

On the other hand, only increased RD in whole ILF (Pattern 1) was sensitive to decreased selectivity for animacy across ventral visual cortex, suggesting that dedifferentiation on a broader scale may be predicted by less severe differences in ILF white matter fibers. Furthermore, we report a significant Age × ILF microstructure interaction (for both FA and

RD), characterized by stronger structure–function coupling in younger adults that weakened with age and was no longer significant after the age of 70 years. White matter in ILF matures through early adulthood, characterized by increased FA and decreased RD, and peaks around ages 26–29 years before beginning to decline (Lebel et al., 2012; Westlye et al., 2010). Furthermore, our sample indicates that ILF degradation becomes more severe after the age of 52 years (Figure 1). Therefore, it is possible that this interaction is capturing the window with the greatest variability in individual differences in white matter maturity (for younger adults) and early and middle stages of white matter degradation (for middle-aged and older adults). That is, optimal white matter microstructure is most predictive of brain function at these transitionary points of the lifespan, but this relationship weakens as white matter aging becomes more prominent.

Interpreting the Current Results in the Context of Prior DTI–fMRI Aging Studies

Prior studies examining the effect of age on the relationship between white matter microstructure and functional activity have largely examined how white matter is related to changes in magnitude or modulation of BOLD response during a cognitive task, with the largest focus on frontal regions of the brain (see Bennett & Rypma, 2013, for a review). Researchers generally report that decreased frontal white matter integrity in older adults corresponds with overactivation of frontal cortex (Daselaar et al., 2015; Hakun et al., 2015; Burzynska et al., 2013; Davis et al., 2012; de Chastelaine et al., 2011; Madden et al., 2007; Persson et al., 2006; but see also de Chastelaine et al., 2011; Davis et al., 2012, for opposite findings), suggesting that the general age phenomenon of increased activity in frontal cortex may be a compensatory response to impaired white matter degradation (Daselaar et al., 2015). White matter degradation in older adults has also been associated with failures to deactivate default regions during task (Brown et al., 2015) and failure to up-modulate prefrontal activity in response to increasing task demands (Webb et al., 2020).

We extend this prior work on higher level cognition by moving our focus to structure–function relationships in ventral visual cortex during a basic perceptual task. Because of the highly organized and hierarchical nature of visual representations in ventral visual cortex (Grill-Spector & Weiner, 2014), we were able to target both focal (i.e., FFA) and broad patterns of specialized functional activity. We report that dedifferentiation of functional response (i.e., less selective response) could be accounted for by decreased FA in underlying white matter at both fine grain and coarse scales. Although this structure–function association can be interpreted as age-independent, examining the unique variance explained by age versus white matter microstructure in our regression models reveals that together these two predictors explained more variance in functional selectivity than on their own, suggesting both age and white matter play an important role. Furthermore, we find evidence for an age-dependent relationship between ILF FA and broad functional selectivity that is not significant in our oldest adults (ages 70+ years). This suggests that intact ILF microstructure is predictive of less dedifferentiated (i.e., more “youth-like”) functional patterns, but only to the point when white matter degradation is not too severe. Our findings, in conjunction with prior DTI–fMRI studies, may indicate that decreased white matter connectivity predicts maladaptive alterations in brain function, be it decreased selectivity, frontal overre-cruitment, or failure to modulate functional activity. Therefore, underlying

white matter structure is an important variable to consider when interpreting age differences in brain function.

Conclusions

In summary, this study offers the first examination of how white matter microstructure (through multiple white matter indices) in the ILF predicts functional selectivity in the ventral visual cortex across the entire adult lifespan. This study provides a comprehensive view of the relationship between measures of white matter microstructure and selectivity in a healthy, aging population, which may help dissociate normal from pathological brain aging in future studies. There are several important points to take away from these findings. First, the effect of white matter on functional selectivity appears to be local, such that neural activity is best predicted by integrity in nearby white matter. Specifically, whole ILF predicts selectivity for animacy across the entire ventral visual cortex, whereas a smaller, proximal region of ILF predicts selectivity for faces in a focal region of fusiform gyrus. Next, coupling between ILF white matter and broad functional selectivity for animacy is not steady across the lifespan—rather, white matter is the strongest predictor of neural selectivity at younger ages, and this relationship weakens but is maintained until the age of 70 years. Future longitudinal studies directly examining intraindividual changes in white matter tracts in relation to functional brain activation are needed to confirm the cross-sectional findings reported here.

Acknowledgments

This study was supported in part by National Institutes of Health Grants R37-AG-006265 (D. C. P.), R37-AG-006265-S1 (D. C. P.), R01-AG-056535 (K. M. K.), and R01-AG-057537 (K. M. R.).

REFERENCES

Barnes CA, & McNaughton BL (1980). Physiological compensation for loss of afferent synapses in rat hippocampal granule cells during senescence. Journal of Physiology, 309, 473–485.

Behrens TE, Berg HJ, Jbabdi S, Rushworth MF, & Woolrich MW (2007). Probabilistic diffusion tractography with multiple fibre orientations: What can we gain? Neuroimage, 34, 144–155. [PubMed: 17070705]

Behrens TE, Woolrich MW, Jenkinson M, Johansen-Berg H, Nunes RG, Clare S, et al. (2003). Characterization and propagation of uncertainty in diffusion-weighted MR imaging. Magnetic Resonance in Medicine, 50, 1077–1088. [PubMed: 14587019]

Bennett IJ, Madden DJ, Vaidya CJ, Howard DV, & Howard JH Jr. (2010). Age-related differences in multiple measures of white matter integrity: A diffusion tensor imaging study of healthy aging. Human Brain Mapping, 31, 378–390. [PubMed: 19662658]

Bennett IJ, Motes MA, Rao NK, & Rypma B (2012). White matter tract integrity predicts visual search performance in young and older adults. Neurobiology of Aging, 33, 433.e21–433.e31.

Bennett IJ, & Rypma B (2013). Advances in functional neuroanatomy: A review of combined DTI and fMRI studies in healthy younger and older adults. Neuroscience & Biobehavioral Reviews, 37, 1201–1210. [PubMed: 23628742]

Brown CA, Hakun JG, Zhu Z, Johnson NF, & Gold BT (2015). White matter microstructure contributes to age-related declines in task-induced deactivation of the default mode network. Frontiers in Aging Neuroscience, 7, 194. [PubMed: 26500549]

Burianová H, Lee Y, Grady CL, & Moscovitch M (2013). Age-related dedifferentiation and compensatory changes in the functional network underlying face processing. Neurobiology of Aging, 34, 2759–2767. [PubMed: 23870836]

Burzynska AZ, Garrett DD, Preuschhof C, Nagel IE, Li SC, Bäckman L, et al. (2013). A scaffold for efficiency in the human brain. Journal of Neuroscience, 33, 17150–17159. [PubMed: 24155318]

Burzynska AZ, Preuschhof C, Bäckman L, Nyberg L, Li SC, Lindenberger U, et al. (2010). Age-related differences in white matter microstructure: Region-specific patterns of diffusivity. Neuroimage, 49, 2104–2112. [PubMed: 19782758]

Carp J, Park J, Polk TA, & Park DC (2011). Age differences in neural distinctiveness revealed by multi-voxel pattern analysis. Neuroimage, 56, 736–743. [PubMed: 20451629]

Catani M, Jones DK, Donato R, & Ffytche DH (2003). Occipito-temporal connections in the human brain. Brain, 126, 2093–2107. [PubMed: 12821517]

de Chastelaine M, Wang TH, Minton B, Muftuler LT, & Rugg MD (2011). The effects of age, memory performance, and callosal integrity on the neural correlates of successful associative encoding. Cerebral Cortex, 21, 2166–2176. [PubMed: 21282317]

Chen NK, Chou YH, Song AW, & Madden DJ (2009). Measurement of spontaneous signal fluctuations in fMRI: Adult age differences in intrinsic functional connectivity. Brain Structure and Function, 213, 571–585. [PubMed: 19727810]

Daselaar SM, Iyengar V, Davis SW, Eklund K, Hayes SM, & Cabeza RE (2015). Less wiring, more firing: Low-performing older adults compensate for impaired white matter with greater neural activity. Cerebral Cortex, 25, 983–990. [PubMed: 24152545]

Davis SW, Dennis NA, Buchler NG, White LE, Madden DJ, & Cabeza R (2009). Assessing the effects of age on long white matter tracts using diffusion tensor tractography. Neuroimage, 46, 530–541. [PubMed: 19385018]

Davis SW, Kragel JE, Madden DJ, & Cabeza R (2012). The architecture of cross-hemispheric communication in the aging brain: Linking behavior to functional and structural connectivity. Cerebral Cortex, 22, 232–242. [PubMed: 21653286]

Ellmore TM, Beauchamp MS, Breier JI, Slater JD, Kalamangalam GP, O'Neill TJ, et al. (2010). Temporal lobe white matter asymmetry and language laterality in epilepsy patients. Neuroimage, 49, 2033–2044. [PubMed: 19874899]

Epstein R, Harris A, Stanley D, & Kanwisher N (1999). The parahippocampal place area: Recognition, navigation, or encoding? Neuron, 23, 115–125. [PubMed: 10402198]

Folstein MF, Folstein SE, & McHugh PR (1975). "Mini-Mental State": A practical method for grading the cognitive state of patients for the clinician. Journal of Psychiatric Research, 12, 189–198. [PubMed: 1202204]

Grady CL, Maisog JM, Horwitz B, Ungerleider LG, Mentis MJ, Salerno JA, et al. (1994). Age-related changes in cortical blood flow activation during visual processing of faces and location. Journal of Neuroscience, 14, 1450–1462. [PubMed: 8126548]

Grill-Spector K, & Malach R (2004). The human visual cortex. Annual Review of Neuroscience, 27, 649–677.

Grill-Spector K, & Weiner KS (2014). The functional architecture of the ventral temporal cortex and its role in categorization. Nature Reviews Neuroscience, 15, 536–548. [PubMed: 24962370]

Gschwind M, Pourtois G, Schwartz S, Van De Ville D, & Vuilleumier P (2012). White-matter connectivity between face-responsive regions in the human brain. Cerebral Cortex, 22, 1564–1576. [PubMed: 21893680]

Hakun JG, Zhu Z, Brown CA, Johnson NF, & Gold BT (2015). Longitudinal alterations to brain function, structure, and cognitive performance in healthy older adults: A fMRI–DTI study. Neuropsychologia, 71, 225–235. [PubMed: 25862416]

Haxby JV, Gobbini MI, Furey ML, Ishai A, Schouten JL, & Pietrini P (2001). Distributed and overlapping representations of faces and objects in ventral temporal cortex. Science, 293, 2425–2430. [PubMed: 11577229]

Haxby JV, Guntupalli JS, Connolly AC, Halchenko YO, Conroy BR, Gobbini MI, et al. (2011). A common, high-dimensional model of the representational space in human ventral temporal cortex. Neuron, 72, 404–416. [PubMed: 22017997]

Haxby JV, Horwitz B, Ungerleider LG, Maisog JM, Pietrini P, & Grady CL (1994). The functional organization of human extrastriate cortex: A PET-rCBF study of selective attention to faces and locations. Journal of Neuroscience, 14, 6336–6353. [PubMed: 7965040]

Johnson PO, & Fay LC (1950). The Johnson-Neyman technique, its theory and application. Psychometrika, 15, 349–367. [PubMed: 14797902]

Kanwisher N, McDermott J, & Chun MM (1997). The fusiform face area: A module in human extrastriate cortex specialized for face perception. Journal of Neuroscience, 17, 4302–4311. [PubMed: 9151747]

Kennedy KM, Hope K, & Raz N (2009). Life span adult faces: Norms for age, familiarity, memorability, mood, and picture quality. Experimental Aging Research, 35, 268–275. [PubMed: 19280451]

Koen JD, & Rugg MD (2019). Neural dedifferentiation in the aging brain. Trends in Cognitive Sciences, 23, 547–559. [PubMed: 31174975]

Kriegeskorte N, Mur M, & Bandettini PA (2008). Representational similarity analysis—Connecting the branches of systems neuroscience. Frontiers in Systems Neuroscience, 2, 4. [PubMed: 19104670]

Lebel C, Gee M, Camicioli R, Wieler M, Martin W, & Beaulieu C (2012). Diffusion tensor imaging of white matter tract evolution over the lifespan. Neuroimage, 60, 340–352. [PubMed: 22178809]

Liu X, Hildebrandt A, Meyer K, Sommer W, & Zhou C (2020). Patterns of individual differences in fiber tract integrity of the face processing brain network support neurofunctional models. Neuroimage, 204, 116229. [PubMed: 31563519]

Madden DJ, Spaniol J, Whiting WL, Bucur B, Provenzale JM, Cabeza R, et al. (2007). Adult age differences in the functional neuroanatomy of visual attention: A combined fMRI and DTI study. Neurobiology of Aging, 28, 459–476. [PubMed: 16500004]

Minear M, & Park DC (2004). A lifespan database of adult facial stimuli. Behavior Research Methods, Instruments, & Computers, 36, 630–633.

O'Toole AJ, Jiang F, Abdi H, & Haxby JV (2005). Partially distributed representations of objects and faces in ventral temporal cortex. Journal of Cognitive Neuroscience, 17, 580–590. [PubMed: 15829079]

O'Toole AJ, Natu V, An X, Rice A, Ryland J, & Phillips PJ (2014). The neural representation of faces and bodies in motion and at rest. Neuroimage, 91, 1–11. [PubMed: 24486831]

Park J, Carp J, Hebrank A, Park DC, & Polk TA (2010). Neural specificity predicts fluid processing ability in older adults. Journal of Neuroscience, 30, 9253–9259. [PubMed: 20610760]

Park J, Carp J, Kennedy KM, Rodrigue KM, Bischof GN, Huang CM, et al. (2012). Neural broadening or neural attenuation? Investigating age-related dedifferentiation in the face network in a large lifespan sample. Journal of Neuroscience, 32, 2154–2158. [PubMed: 22323727]

Park DC, Polk TA, Park R, Minear M, Savage A, & Smith MR (2004). Aging reduces neural specialization in ventral visual cortex. Proceedings of the National Academy of Sciences, U.S.A, 101, 13091–13095.

Park DC, & Reuter-Lorenz P (2009). The adaptive brain: Aging and neurocognitive scaffolding. Annual Review of Psychology, 60, 173–196.

Persson J, Nyberg L, Lind J, Larsson A, Nilsson L-G, Ingvar M, et al. (2006). Structure–function correlates of cognitive decline in aging. Cerebral Cortex, 16, 907–915. [PubMed: 16162855]

Preacher KJ, Curran PJ, & Bauer DJ (2006). Computational tools for probing interactions in multiple linear regression, multilevel modeling, and latent curve analysis. Journal of Educational and Behavioral Statistics, 31, 437–448.

Proklova D, Kaiser D, & Peelen MV (2016). Disentangling representations of object shape and object category in human visual cortex: The animate–inanimate distinction. Journal of Cognitive Neuroscience, 28, 680–692. [PubMed: 26765944]

Pyles JA, Verstynen TD, Schneider W, & Tarr MJ (2013). Explicating the face perception network with white matter connectivity. PLoS One, 8, e61611. [PubMed: 23630602]

Rieck JR, Rodrigue KM, Kennedy KM, Devous MD, & Park DC (2015). The effect of beta-amyloid on face processing in young and old adults: A multivariate analysis of the BOLD signal. Human Brain Mapping, 36, 2514–2526. [PubMed: 25832770]

Sasson E, Doniger GM, Pasternak O, & Assaf Y (2010). Structural correlates of memory performance with diffusion tensor imaging. Neuroimage, 50, 1231–1242. [PubMed: 20045476]

Saygin ZM, Osher DE, Koldewyn K, Reynolds G, Gabrieli JD, & Saxe RR (2012). Anatomical connectivity patterns predict face selectivity in the fusiform gyrus. Nature Neuroscience, 15, 321–327.

Sha L, Haxby JV, Abdi H, Guntupalli JS, Oosterhof NN, Halchenko YO, et al. (2014). The animacy continuum in the human ventral vision pathway. Journal of Cognitive Neuroscience, 27, 665–678. [PubMed: 25269114]

Tavor I, Yablonski M, Mezer A, Rom S, Assaf Y, & Yovel G (2014). Separate parts of occipito-temporal white matter fibers are associated with recognition of faces and places. Neuroimage, 86, 123–130. [PubMed: 23933304]

Thomas C, Moya L, Avidan G, Humphreys K, Jung KJ, Peterson MA, et al. (2008). Reduction in white matter connectivity, revealed by diffusion tensor imaging, may account for age-related changes in face perception. Journal of Cognitive Neuroscience, 20, 268–284. [PubMed: 18275334]

Turken U, Whitfield-Gabrieli S, Bammer R, Baldo JV, Dronkers NF, & Gabrieli JDE (2008). Cognitive processing speed and the structure of white matter pathways: Convergent evidence from normal variation and lesion studies. Neuroimage, 42, 1032–1044. [PubMed: 18602840]

Tzourio-Mazoyer N, Landeau B, Papathanassiou D, Crivello F, Etard O, Delcroix N, et al. (2002). Automated anatomical labeling of activations in spm using a macroscopic anatomical parcellation of the MNI MRI single-subject brain. Neuroimage, 15, 273–289. [PubMed: 11771995]

Warbrick T, Rosenberg J, & Shah NJ (2017). The relationship between BOLD fMRI response and the underlying white matter as measured by fractional anisotropy (FA): A systematic review. Neuroimage, 153, 369–381. [PubMed: 28082105]

Webb CE, Hoagey DA, Foster CM, Rodrigue KM, & Kennedy KM (2020). Contributions of BOLD modulation and white matterdiffusivity to cognitiveaging: A lifespan SEM study. Cerebral Cortex. 10.1093/cercor/bhz193.

Weiner KS, Jonas J, Gomez J, Maillard L, Brissart H, Hossu G, et al. (2016). The face-processing network is resilient to focal resection of human visual cortex. Journal of Neuroscience, 36, 8425–8440. [PubMed: 27511014]

Westlye LT, Walhovd KB, Dale AM, Bjornerud A, Due-Tonnessen P, Engvig A, et al. (2010). Life-span changes of the human brain white matter: Diffusion tensor imaging (DTI) and volumetry. Cerebral Cortex, 20, 2055–2068. [PubMed: 20032062]

Yeatman JD, Dougherty RF, Myall NJ, Wandell BA, & Feldman HM (2012). Tract profiles of white matter properties: Automating fiber-tract quantification. PLoS One, 7, e49790. [PubMed: 23166771]

Yeh FC, Badre D, & Verstynen T (2016). Connectometry: A statistical approach harnessing the analytical potential of the local connectome. Neuroimage, 125, 162–171. [PubMed: 26499808]

Zhu Z, Johnson NF, Kim C, & Gold BT (2015). Reduced frontMal cortex efficiency is associated with lower white matter integrity in aging. Cerebral Cortex, 25, 138–146. [PubMed: 23960206]

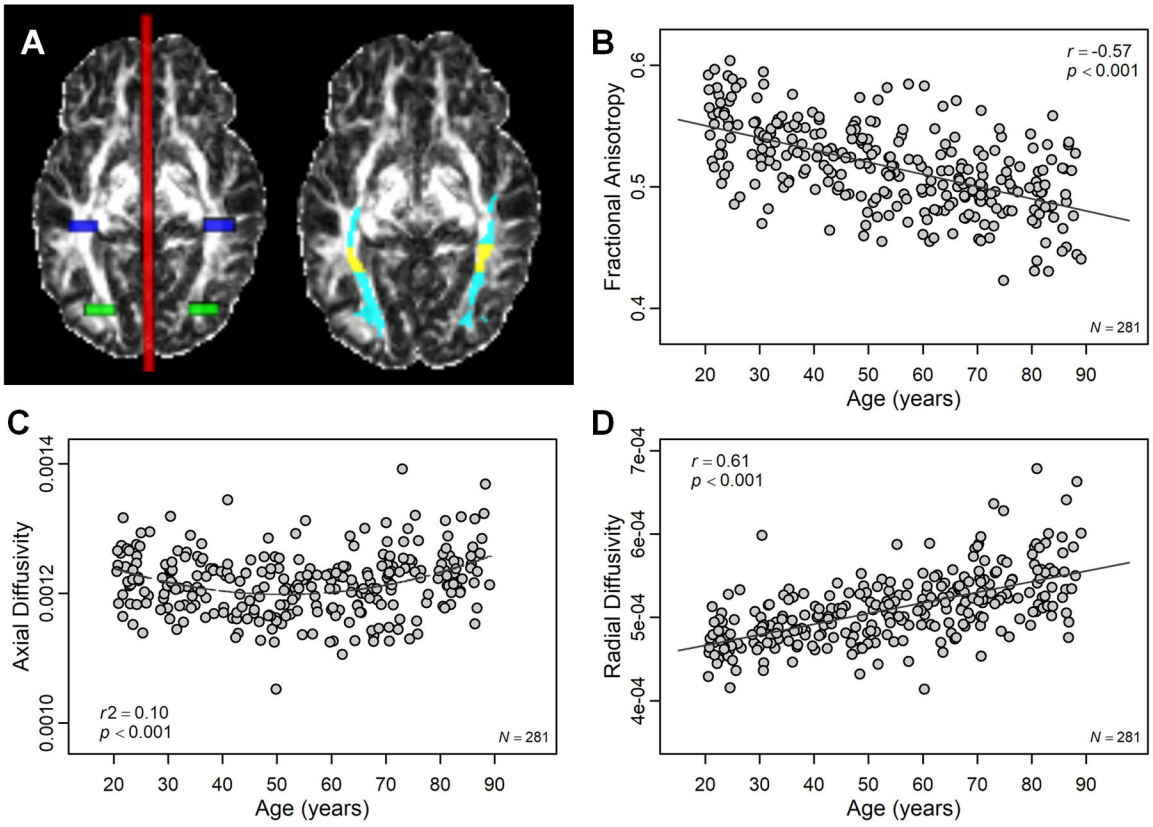

Figure 1.

Effect of age on white matter diffusion metrics in ILF. (A) Seed (green), waypoint (blue), and exclusion (red) masks used for probabilistic tractography of left and right ILF (left side) as well as the resulting ILF tract (cyan; right side) are illustrated for a representative participant. Mid-fusiform ILF has been highlighted in yellow. (B) With increasing age, diffusivity in ILF was more isotropic (i.e., lower FA), which was characterized by (C) nonlinear age differences in AD and (D) linear age increases in RD.

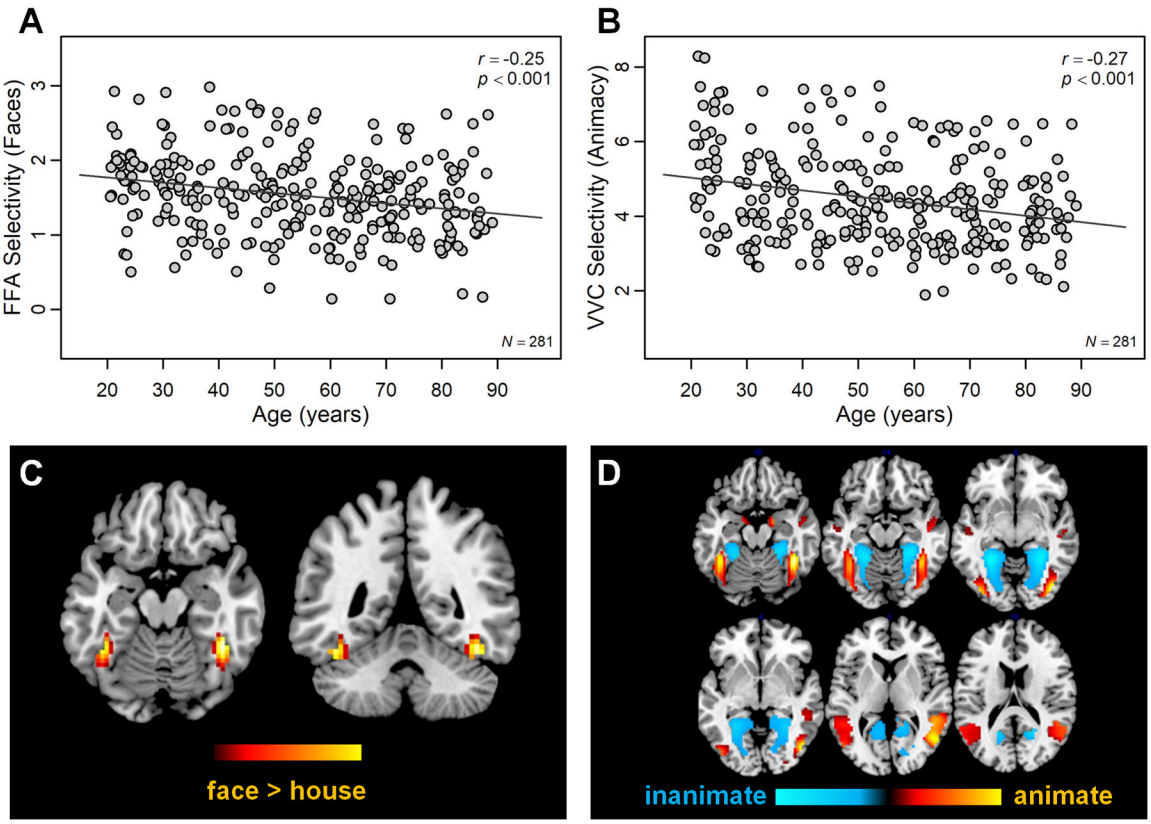

Figure 2.

Effect of age on functional selectivity. (A) With increasing age, selectivity for faces in FFA decreased. (B) Likewise, selectivity for animacy across ventral visual cortex decreased. Functional activation maps illustrate (C) FFA and (D) activity associated with viewing animate versus inanimate images mapped to a common template space.

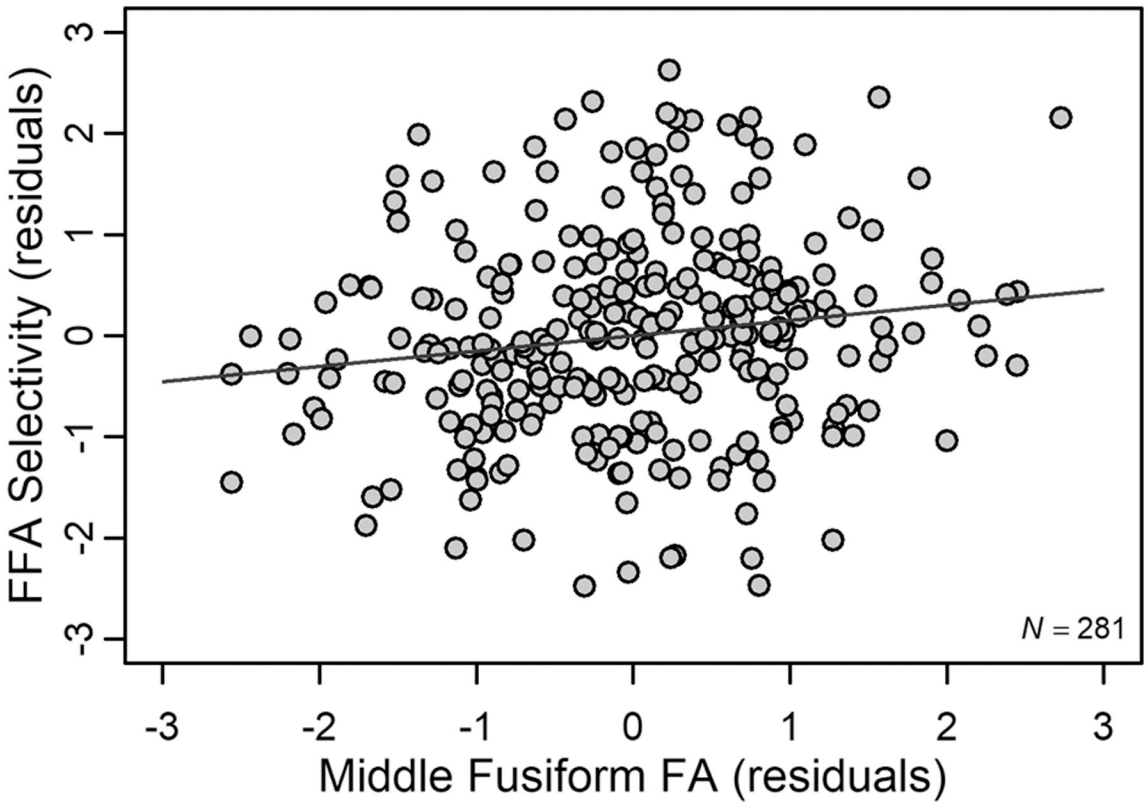

Figure 3.

Effect of mid-fusiform FA on FFA selectivity. Increased FA in a portion of middle fusiform ILF corresponded to increased face selectivity in FFA. Standardized residuals (after accounting for age and other white matter tracts) are plotted for middle fusiform FA and FFA selectivity.

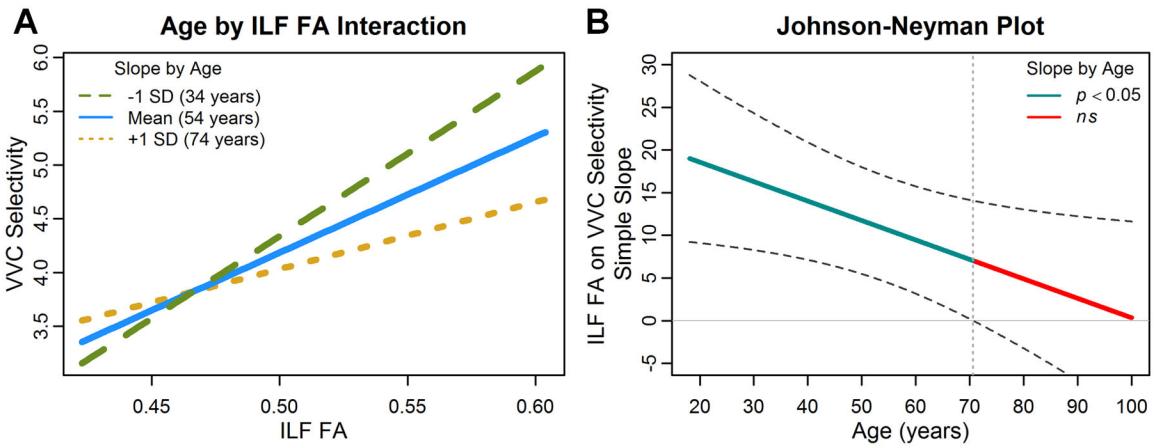

Figure 4.

Effect of ILF FA on ventral visual selectivity to animacy depends on age. (A) Increased FA in whole ILF corresponded to increased selectivity for animacy across ventral visual cortex (VVC). However, this relationship weakened with age, as evident by plotting the slope of the relationship between ILF FA and VVC selectivity for the sample mean age (54 years; solid blue line) and 1 *SD* above (74 years; dotted yellow line) and 1 *SD* below (34 years; dashed green line). (B) The Johnson–Neyman plot illustrates the structure–function slopes at each point of the lifespan with 95% confidence intervals (dashed lines) indicating that the ILF FA and VVC selectivity relationship was no longer significant after the age of 70 years (where the confidence intervals cross 0, delineated with a vertical dotted line).

Table 1.

Sample Demographics by Decade

Age Range	n (% Female)	Age	Years of Education	MMSE
20–29	41 (65.9%)	24.37 (2.78)	15.95 (2.32)	28.90 (1.26)
30–39	40 (60.0%)	34.06 (2.83)	16.85 (2.35)	28.63 (1.17)
40–49	41 (65.9%)	45.41 (3.19)	15.82 (1.99)	28.54 (1.19)
50–59	37 (73.0%)	54.63 (2.87)	16.89 (2.20)	28.76 (.925)
60–69	43 (58.1%)	64.82 (2.88)	16.88 (2.16)	28.21 (1.25)
70–79	39 (66.7%)	73.34 (2.75)	16.23 (2.40)	28.00 (1.29)
80–89	40 (60.0%)	83.65 (2.66)	16.28 (2.35)	27.30 (1.11)
20–89 (whole sample)	281 (64.1%)	54.23 (19.99)	16.41 (2.27)	28.33 (1.27)

Data were analyzed with age as a continuous variable in all analyses. Values in the table represent mean (standard deviation). MMSE = Mini-Mental State Examination.

Table 2.

Regression Models: Predicting Selectivity for Faces in FFA

Model	Steps	Measurement	R^2	ΔR^2	ΔR^2 p	F	P	η^2
A. FA								
1	1	Age	.062	—	—			
2	1	Age	.068	.006	.797			
	2	Other white matter FA (SLF, UF, genu, splenium)						
3	1	Age	.070	.002	.421			
	2	Other white matter FA						
	3	Whole ILF FA						
4	1	Age	.092	.022	.012	1.73	.001	.038
	2	Other white matter FA				all < 1	all > .1	all < .003
	3	Whole ILF FA				2.02	.156	.007
	4	Middle fusiform ILF FA				6.43	.012	.023
B. RD								
1	1	Age	.095	—	—	14.73	< .001	.051
		Other white matter RD				all < 1	all > .1	all < .007
		Whole ILF RD				2.84	.093	.010
		Middle fusiform ILF RD				3.97	.047	.015
C. AD								
1	1	Age	.099	—	—	< 1	.588	.001
		Other white matter AD				all < 1	all > .1	all < .001
		Whole ILF AD				<1	.619	.015
		Middle fusiform ILF AD				15.24	< .001	.053

F, *p*, and η^2 are reported for the highest step significant regression models; other white matter pathways (SLF, UF, genu, and splenium) were entered as separate predictors.

Table 3.

Regression Models: Predicting Selectivity for Animacy across Ventral Visual Cortex

Model	Steps	Measurement	R^2	ΔR^2	ΔR^2 p	F	P	η^2
A. FA								
1	1	Age	.071	—	—	—	—	—
2	1	Age	.077	.006	.788			
	2	Other white matter FA (SLF, UF, genu, splenium)						
3	1	Age	.078	.001	.583			
	2	Other white matter FA						
	3	Ventral visual cortex size						
4	1	Age	.115	.037	.001			
	2	Other white matter FA						
	3	Ventral visual cortex size						
	4	ILF FA						
5	1	Age	.130	.015	.031	*3.75*	*.054*	*.014*
	2	Other white matter FA				all < 1	all > .1	all < .008
	3	Ventral visual cortex size				<1	.545	.001
	4	ILF FA				12.44	<.001	.044
	5	Age × ILF FA				4.66	.032	.017
B. RD								
1	1	Age	.137	—	—	5.90	.016	.021
		Other white matter RD				all < 1	all > .1	all < .004
		Ventral visual cortex size				<1	.395	.003
		ILF RD				10.52	.001	.037
		Age × ILF RD				4.51	.035	.016
C. AD								
1	1	Age	.118	—	—	25.40	< .001	.085
		Other white matter AD				all < 1	all > .1	all < .003
		Ventral visual cortex size				<1	.967	< .001
		ILF AD				<1	.527	.002
		Age × ILF AD				<1	.762	< .001

F, *p*, and η^2 are reported for the highest step significant regression models; other white matter pathways (SLF, UF, genu, and splenium) were entered as separate predictors.